RESEARCH ARTICLE

MRI Extracellular Volume Fraction in Liver Fibrosis—A Comparison of Different Time Points and Blood Pool Measurements

Verena Carola Obmann, MD,[1,2] Marie Ardoino, MMed,[1] Jeremias Klaus, MD,[1,3] Damiano Catucci, MD,[1,4] Annalisa Berzigotti, MD,[5] Matteo Montani, MD,[6] Alan Peters, MD,[1] Inga Todorski, MD,[1] Benedikt Wagner, MD,[1] Lukas Zbinden, MSc, PhD Student,[1,7] Christoph Gräni, MD, PhD,[8] Lukas Ebner, MD,[1,9] Johannes Thomas Heverhagen, MD, PhD,[1] Andreas Christe, MD,[1,2] and Adrian Thomas Huber, MD, PhD[1,2,9*]

Background: Extracellular volume (ECV) correlates with the degree of liver fibrosis.
Purpose: To analyze the performance of liver MRI-based ECV evaluations with different blood pool measurements at different time points.
Study Type: Prospective.
Sample: 73 consecutive patients ($n = 31$ females, mean age 56 years) with histopathology-proven liver fibrosis.
Field Strength/Sequence: 3T acquisition within 90 days of biopsy, including shortened modified look–locker inversion recovery T1 mapping.
Assessment: Polygonal regions of interest were manually drawn in the liver, aorta, vena cava, and in the main, left and right portal vein on four slices before and after Gd-DOTA administration at 5/10/15 minutes. ECV was calculated 1) on one single slice on portal bifurcation level, and 2) averaged over all four slices.
Statistical Tests: Parameters were compared between patients with fibrosis grades F0-2 and F3-F4 with the Mann–Whitney U and fishers exact test. ROC analysis was used to assess the performance of the parameters to predict F3-4 fibrosis. A *P*-value <0.05 was considered statistically significant.
Results: ECV was significantly higher in F3-4 fibrosis (35.4% [33.1%–37.6%], 36.1% [34.2%–37.5%], and 37.0% [34.8%–39.2%] at 5/10/15 minutes) than in patients with F0-2 fibrosis (33.3% [30.8%–34.8%], 33.7% [31.6%–34.7%] and 34.9% [32.2%–36.0%]; AUC = 0.72–0.75). Blood pool T1 relaxation times in the aorta and vena cava were longer on the upper vs. lower slices at 5 minutes, but not at 10/15 minutes. AUC values were similar when measured on a single slice (AUC = 0.69–0.72) or based on blood pool measurements in the cava or portal vein (AUC = 0.63–0.67 and AUC = 0.65–0.70).
Data Conclusion: Liver ECV is significantly higher in F3-4 fibrosis compared to F0-2 fibrosis with blood pool measurements performed in the aorta, inferior vena cava, and portal vein at 5, 10, and 15 minutes. However, a smaller variability was observed for blood pool measurements between slices at 15 minutes.
Level of Evidence: 1
Technical Efficacy: Stage 3

J. MAGN. RESON. IMAGING 2024.

View this article online at wileyonlinelibrary.com. DOI: 10.1002/jmri.29259

Received Oct 25, 2023, Accepted for publication Jan 14, 2024.

*Address reprint requests to: A.H., Department of Diagnostic, Interventional and Pediatric Radiology, Freiburgstrasse 10, Inselspital, 3010 Bern, Switzerland.
E-mail: adrian.huber@insel.ch

From the [1]Department of Diagnostic, Interventional and Pediatric Radiology, Inselspital Bern, University Hospital, University of Bern, Bern, Switzerland; [2]Liver Elastography Center, Translational Imaging Center (TIC), Swiss Institute for Translational and Entrepreneurial Medicine, Bern, Switzerland; [3]Institute of Forensic Medicine, University of Bern, Bern, Switzerland; [4]Graduate School for Health Sciences, University of Bern, Bern, Switzerland; [5]Department of Visceral Surgery and Medicine, Inselspital Bern University Hospital, University of Bern, Bern, Switzerland; [6]Department of Pathology, University of Bern, Bern, Switzerland; [7]ARTORG Center for Biomedical Engineering Research, University of Bern, Bern, Switzerland; [8]Department of Cardiology, Inselspital, Bern University Hospital, University of Bern, Bern, Switzerland; and [9]Radiology and Nuclear Medicine (RUN), Luzerner Kantonsspital, University of Lucerne, Switzerland, Lucerne, Switzerland

Additional supporting information may be found in the online version of this article

Liver fibrosis shows a high morbidity with the risk of hepatic decompensation and hepatocellular carcinoma in advanced stages.[1] Early detection and treatment in precirrhotic, reversible stages are therefore warranted.[2] The reference standard to stage liver fibrosis is liver biopsy, which is limited to selected patients due to its invasiveness.[3] Noninvasive methods such as serum markers and morphologic parameters in ultrasound, computed tomography,[4,5] and MRI[6] have a limited accuracy, especially in early, precirrhotic stages of liver fibrosis. Ultrasound shear wave elastography and transient elastography allow to accurately stage fibrosis but do have several limitations such as operator dependence, problems in obese patients, a narrow window of measurement, shallow measurement depth of only a small focal part of the liver and in case of transient elastography no correlating real time b-mode image.[7,8] Other than clinical information and serum markers, ultrasound measurements are not always available at the time of liver MRI. In addition, all those methods have limitations to grade early fibrosis stages.[9] More recently, MR elastography (MRE) showed high accuracy in grading liver fibrosis and is now considered as the noninvasive reference standard to grade liver fibrosis.[10–12] However, MRE needs expensive additional hardware and is not yet widely available. Consequently, MRI sequences without requiring additional hardware are therefore needed for multiparametric MRI assessment of the liver.

Quantitative MRI T1 mapping has been associated with liver fibrosis, but also with liver inflammation and fat, and is dependent on the MRI field strength.[6] A combination of T1 relaxation time measurements in the liver and blood pool before and after injection of an extracellular contrast agent allows calculation of the extracellular volume (ECV).[13,14] The ECV represents the tissue volume that is not taken by the cells and may therefore be less prone to the confounding inflammation and fat.[15]

The ECV is expanded in liver cirrhosis due to extracellular fibrosis and decreased hepatocellular volume, which has been shown to correlate well with the degree of fibrosis in histology in different organs, such as the myocardium and the liver.[16,17] The underlying hypothesis is that an extracellular Gadolinium-based agent is equally distributed to the blood pool and the liver extracellular space in equilibrium phase.[18] Preclinical animal studies have shown increased ECV in liver fibrosis.[14,19] Few clinical data exist, mainly from the group of Jin and Wang et al in hepatitis B patients[18,20] and Mesropyan et al in patients with autoimmune hepatitis (AIH) and primary sclerosing cholangitis.[21,22] All those studies used the abdominal aorta for blood pool measurements. However, no data exist comparing measurements in different blood pools, including the aorta, but also the inferior vena cava (IVC) and the portal vein, which are closer to the liver. The liver has a dual blood supply and receives the majority of their nutritions by the portal vein and drains through the liver veins into the IVC. For this reason it might be possible that the location of the measured bloodpool might have impact on the liver ECV calculation.

In addition, clinical data with ECV measurements at different time points and direct comparisons with histology are missing. As it is known that the liver equilibrium phase can be reached as soon as 3 minutes after contrast injection it might be possible that the best time point for ECV calculation is earlier than used in previous studies.[23] Further, a calculation of ECV using earlier post contrast aquistions would allow better implementation into more and more time restricted clinical MRI protocols and thus the clinical use of ECV as a cheap promising non invasive liver fibrosis biomarker.

Against this background, the aim of our study was to analyze the performance of liver MRI ECV fraction assessment with different blood pool measurements and time points in comparison to the grade of liver fibrosis on histopathology in patients with chronic liver disease.

Materials and Methods

This prospective study was approved by the local institutional review board and was carried out in accordance with the principles of the Declaration of Helsinki. Written informed consent was obtained from all patients.

Sample

Patients undergoing liver biopsy for grading and staging of chronic liver disease (any etiology) in our institution were consecutively and prospectively enrolled between 08/2018 and 03/2023. All participants underwent a multiparametric MRI with T1 mapping within a maximum of 90 days between liver biopsy and MRI. The following patients were excluded: those with incomplete MRI exams due to claustrophobia, iron overload, previous liver surgery, or multiple focal liver lesions, potentially biasing correct liver T1 relaxation time measurements. In addition, patients who were unable to undergo MRI within 90 days of liver biopsy during the coronavirus disease of 2019 (COVID-19) pandemia were excluded.

Histopathologic Evaluation

Liver biopsies were evaluated with disease-specific pathology grading systems. For metabolism-associated steatosis liver disease (MASLD) patients, the steatosis, activity, fibrosis scoring as described by Bedossa et al was performed.[24] For the remaining liver etiologies, the meta-analysis of histological data in viral hepatitis fibrosis grading system was used[25] by one pathologist with 15 years experience with liver histopathology (M.M.) blinded to the MRI findings.

Clinical Evaluation

All patients underwent clinical evaluation including detailed medical history (especially alcoholic consumption, height, weight, history of diabetes or hypertension, and relevant comorbidities) and laboratory tests including liver parameters (AST, aspartate aminotransferase; ALT, alanine aminotransferase; GGT, gamma-glutamyltransferase; bilirubine; and albumin), platelets and creatinine. Hematocrit

measurements were additionally performed on the day of the MRI examination. Biochemical fibrosis indices such as fibrosis 4 (FIB-4) score and AST to platelet ratio index (APRI) were calculated for all patients. Liver stiffness measurements with transient elastography were performed (Fibroscan®, Echosens, Paris, France).

MRI Technique

All liver exams were performed on a 3-T MRI system (Prisma; Siemens Healthineers, Erlangen, Germany) in a fasting state (>6 h) including T1- and T2-weighted and Q-DIXON sequences to calculate the proton density fat fraction (PDFF), T1 relaxometry. For T1 relaxometry, four single breath-hold (11 msec) axial slices with an equal spacing of 300% (24 mm) between slices were acquired for the liver within a total scan time of 1 minute 37 seconds using a modified look–locker inversion recovery (MOLLI) variant sequence with a 3–3-5 design. Patients' electrocardiogram was simulated by pulse triggering on the patient's fingertip. The following parameters were used: repetition time (TR) of 740 msec, echo time (TE) of 1.01 msec, inversion time (TI) of 225 msec (three inversion pulses at 65 msec, 145 msec, and 225 msec), and flip angle of 35°. The TR of the bSSFP readout pulse (echo spacing) was 2.7 msec. The slice thickness was 8 mm, the field of view was 306 × 360 mm, and the matrix was 154 × 192 pixels. The T1 maps were acquired before and 5, 10, and 15 minutes after intravenous injection of 0.1 mmol gadoteric acid/kg bodyweight (Dotarem, 0.5 mmol/mL; Guerbet, Villepinte, France).

Image Analysis

Polygonal regions of interest (ROIs) were manually drawn in the liver by one radiologist (9 years of experience in hepatic imaging, V.O.) blinded to the histopathological results on T1 maps before and 5, 10, and 15 minutes after contrast agent administration in the Picture Archiving and communication System or our hospital (IDS7, Sectra, Linköping, Sweden). The ROIs for all four slices of each acquisition were measured with a minimal distance of 5 mm to the liver border and to large blood vessels to avoid partial volume effects. Large blood vessels were defined as liver veins and main and segmental portal vein branches, which were visible on the precontrast T1 map. Liver areas directly adjacent to the lung on the upper anterior and posterior liver borders were excluded to avoid partial volume and air susceptibility effects,[6] as illustrated in Fig. 1.

For the blood pool T1 measurements, ROIs were set in the aorta, in the portal vein, and in the IVC on each slice, if possible. Anatomical location ranged for the upper liver level to the lower liver level. For the IVC, this resulted in measurements above the liver vein confluence on the upper slice and below on the lower slices. The portal vein was measured in the common trunk between the confluence and bifurction on the lower slices and in the central left or right portal vein branch on the upper slices. The aorta was measured on four slices covering the supradiaphragmatic up to the infrarenal aorta. Thus, the anatomical location ranged from the upper to the lower liver level. The maximal measurable vessel content was contured avoiding artefacts and vessel walls, especially calcifications of the aortic wall, resulting in a polygonal shape. As the liver has a dual arterial and venous blood supply, a fourth blood pool measurement was synthesized with a compound weighted measurement of 30% in the aorta and 70% in the portal vein. To compare differences in blood pool T1 relaxation times between different levels, the measured values from the two upper slices (upper level) and the two lower slices (lower level) were averaged in the aorta and the portal vein. Similarly, the values in the IVC were averaged above (upper level) and below (lower level) the liver vein confluens.

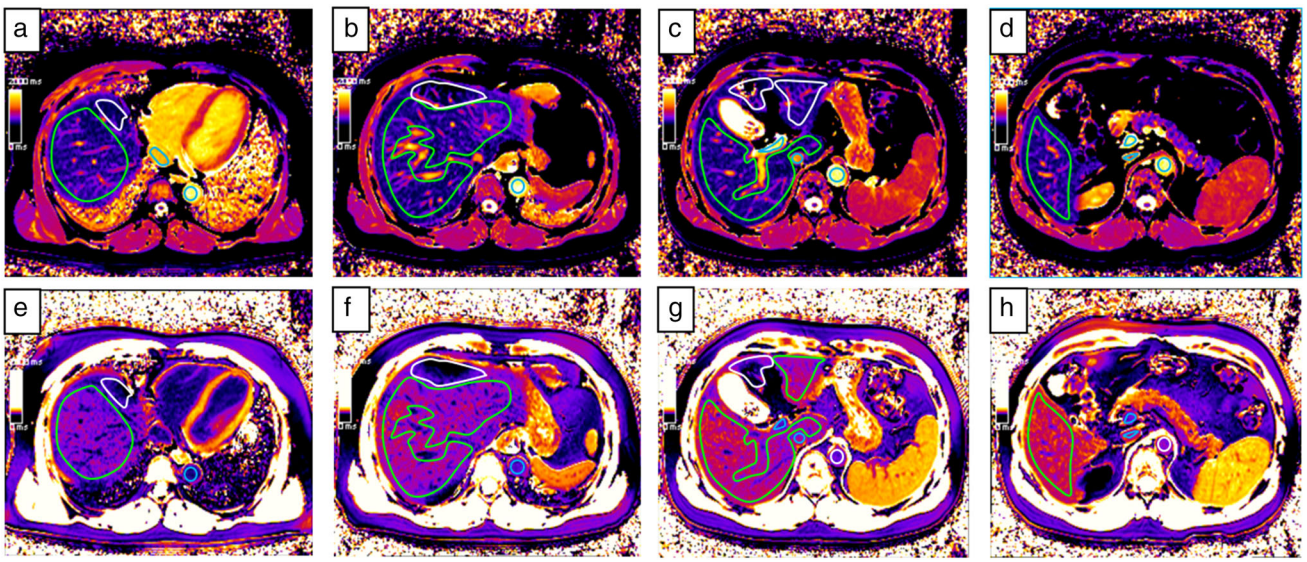

FIGURE 1: T1 relaxation time measurements in the liver and the aorta of a 49-year-old male patient without liver fibrosis (F0). Measurements are shown on (a–d) four consecutive slices on the noncontrast acquisitions and (e–h) four consecutive slices 5 minutes after contrast agent administration. While T1 relaxation times in the liver and aorta did not differ between slices on the noncontrast acquisitions, a T1 shortening effect between slices may occur on early 5 minutes acquisitions after contrast medium administration, due to the time delay between acquisitions of the slices. This time-dependent T1 shortening effect early after contrast agent administration may be observed between (e,f) upper and (g,h) lower slices 5 minutes after contrast agent administration, visualized by the color change from purple to pink. ROIs that were used for liver and vessel T1 measurements are shown in white and blue. Areas with technical artifacts (b,c,e,f) or partial volume (g) where we could not measure are highlighted in red.

Based on normalization to the blood pool, the liver ECV was calculated by dividing the difference of the relaxation rates in the liver and blood pool before and after contrast medium administration. As the blood pool ECV is known (1-hematocrit), it may be multiplied with this ratio to calculate the liver ECV using the following formula[26,27]:

$$ECV = \frac{\left(\frac{1}{T1}\text{liver postcontrast} - \frac{1}{T1}\text{liver precontrast}\right)}{\left(\frac{1}{T1}\text{blood postcontrast} - \frac{1}{T1}\text{blood precontrast}\right)} \text{x}(1 - \text{hematocrit})$$

For single-slice ECV measurements, liver parenchyma and blood pool were measured on one slice at the level of the portal vein bifurcation. For mean ECV measurements, liver parenchyma and blood pool measurements were measured on all four slices and the weighted average depending on the liver ROI size in pixels was used.

$$\begin{aligned}\text{ECV mean} = &((\text{ECV slice } 1 * \text{Pixel } 1) \\ &+ (\text{ECV slice } 2 * \text{Pixel } 2) \\ &+ (\text{ECV slice } 3 * \text{Pixel } 3) \\ &+ (\text{ECV slice } 4 * \text{Pixel } 4))/(\text{Pixel } 1 + 2 + 3 + 4)\end{aligned}$$

For reproducibility analysis (to show that ECV measurements are reader independent and reproducible), ECV with the different blood pool measurements were assessed by a second reader with 2 years experience in liver MRI (D.C.). Twenty randomly selected liver MRI (10 with fibrosis F0-2 and 10 with F3-4) were reassessed. For PDFF assessment liver ROI were drawn on the fat fraction map of the q-dixon sequence.

Statistical Analysis

Analysis was performed with the statistical software package R (version 3.4.1; https://www.r-project.org/)[28] and GraphPad Prism (version 7.1; GraphPad Software Inc., San Diego, CA, USA). Clinical characteristics were compared between groups with early and advanced liver fibrosis corresponding to liver fibrosis grades F0-2 and F3-F4,[29] using the Wilcoxon test for continuous variables or Fisher's exact test for categorical variables. The T1 relaxation times were compared between upper and lower slices in the different blood pool locations (aorta, IVC, portal vein) with the Mann–Whitney test for different time points (noncontrast, as well as 5, 10, and 15 minutes after contrast agent administration).

The ECV was compared between patients with early (F0-2) and advanced (F3-4) liver fibrosis with different blood pool measurements and at different time points (5, 10, and 15 minutes after contrast agent administration) with a Mann–Whitney test and a receiver operating characteristic (ROC) analysis. Delong test was performed to compare area under the curve (AUC) values. To compare ECV results also ROC analysis for PDFF, APRI, and FIB-4 scores as well as a comined analysis of these scores with ECV discriminating F0-2 from F3-4 have been performed.

For reproducibility analysis inter-rater analysis was performed and therefore intraclass correlation coefficients (ICCs) calculated, using a two-way mixed model. An ICC below 0.5 was defined as poor, 0.5–0.75 as moderate, 0.75–0.90 as good, and above 0.90 as excellent.[30] For all statistical tests, a *P*-value of <0.05 was considered statistically significant.

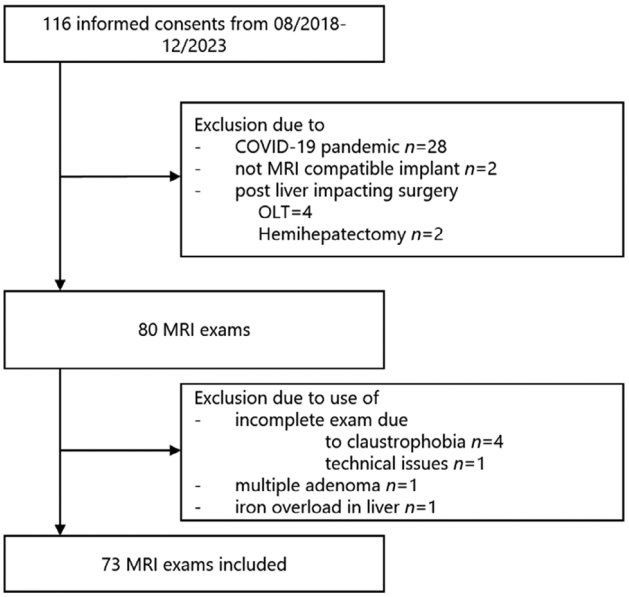

FIGURE 2: Study inclusion flowchart. A total of 116 patients with liver biopsy were prospectively enrolled to undergo an MRI. Twenty-eight MRI had to be annulated because of the COVID-19 pandemic. Two more patients had to excluded because of MRI incompatible implants and six patients were excluded because of prior liver surgery. From 80 MRI, 3 were excluded because of liver iron overload, multiple liver lesions and four scans were not complete due to claustrophobia.

Results

Patient Characteristics

A total of 80 patients with liver biopsy were prospectively enrolled to undergo multiparametric liver MRI. Seven patients were excluded because of an incomplete MR exam due to claustrophobia ($n = 4$), technical issues ($n = 1$), iron overload ($n = 1$), or multiple adenomas ($n = 1$; Fig. 2). From the resulting final patient population, 42 patients had no or early liver fibrosis (F0 = 9, F1 = 10, and F2 = 23) and 31 had advanced liver fibrosis (F3 = 26 and F4 = 5).

The most frequent liver fibrosis etiology was MAFLD/MASLD (Table 1). Patients with advanced liver fibrosis (F3-4) had significantly higher FIB-4 scores (2.5 vs. 1.4), APRI scores (0.68 vs. 0.43) and bilirubin values (11.5 vs. 9.0) than patients with early liver fibrosis (F0-2) and significant lower ALT values (44.0 vs. 77.0) (Table 2). There was no significant difference regarding BMI (28.9 vs. 27.3, $P = 28$), presence of type 2 diabetes mellitus (36% vs. 26%, $P = 44$), or arterial hypertension (42% vs. 48%, $P = 64$) between groups (Table 2).

TABLE 1. Etiology Liver Disease

Etiology	F0-2 ($n = 42$)	F3-4 ($n = 31$)	*P*-value
MAFLD	26 (62%)	16 (52%)	0.47
ARLD	3 (7%)	7 (23%)	0.08
Viral hepatitis (B/C)	6 (14%)	3 (10%)	0.72
PSC/PBC	0 (0%)	2 (6%)	0.18
Autoimmunhepatitis	3 (7%)	1 (3%)	0.63
Other	4 (10%)	2 (6%)	0.99

MAFLD = metabolic associated fatty liver disease; ARLD = alcohol related liver disease; PSC = Primary sclerosing cholangitis; PBC = Primary biliary cholangitis.

TABLE 2. Patient Characteristics

	F0-2	*n*	F3-4	*n*=	*P*-value
Age (years)	54 [46–62]	42	61 [50–71]	31	0.0335
Male, *n* (%)	27 (64.3%)	42	15 (48%)	31	0.2322
Alcohol consumption, *n* (%)	6 (14.3%)	42	4 (12.9%)	31	>0.9999
Diabetes, *n* (%)	11 (26.2%)	42	11 (35.5%)	31	0.4454
Hypertension, *n* (%)	20 (47.6%)	42	13 (41.9%)	31	0.6437
BMI (kg/m^2)	27.3 [24.8–32.9]	42	28.9 [26.1–32.8]	31	0.2821
PDFF (%)	7.8 [2.9–17.3]	42	10.0 [3.2–15.3]	31	0.8701
AST (U/L)	35.0 [27.0–52.8]	42	50.0 [31.0–79.0]	31	0.0871
ALT (U/L)	77.0 [59.8–103.0]	42	44.0 [28.0–81.0]	31	<0.001
GGT (U/L)	68.5 [39.5–138.8]	42	107.0 [47.0–225.0]	31	0.1077
Alkaline phosphatase (U/L)	53.5 [33.8–87.0]	42	96.0 [58.0–132.0]	31	<0.001
Bilirubin (µmol/L)	9.0 [7.0–12.0]	41	11.5 [8.8–18.0]	30	0.0198
Albumin (g/L)	38.0 [36.0–41.0]	39	37.5 [33.0–40.0]	30	0.4442
Platelets (10^9/L)	221.5 [180.8–263.5]	42	186.0 [153.0–253.0]	31	0.0915
APRI	0.43 [0.28–0.71]	42	0.68 [0.38–1.18]	31	0.0213
FIB-4	1.27 [0.96–1.80]	42	2.59 [1.48–3.32]	31	<0.001
Creatinine (µmol/L)	74.0 [60.8–84.0]	42	70.0 [60.0–86.0]	31	0.6671

T1 Mapping ROI

The mean ROI size of T1 relaxation time measurements in the liver was 3276 ± 1799 pixels.

T1 Mapping of Different Vessels

Noncontrast T1 relaxation times did not significantly differ between upper and lower slices in the aorta ($P = 0.86$), portal vein ($P = 0.35$), and IVC ($P = 0.29$) (Table 3). Early 5 minutes after contrast medium administration, T1 relaxation times of the IVC were significantly shorter above the liver vein confluens than below the liver vein confluens (Table 3) and also in the upper versus the lower slices of the aorta. For all other time points, no significant difference for T1 relaxation times in the upper and lower slices of the portal vein was observed (5 minutes $P = 0.25$, 10 minutes $P = 0.47$, 15 minutes $P = -67$, Table 3).

TABLE 3. T1 Relaxation Times of the Blood Pool

	Noncontrast	Contrast 5 minutes	Contrast 10 minutes	Contrast 15 minutes
Aorta				
Upper slices (msec)	1894 [1839–1955]	359 [329–398]	514 [486–546]	591 [560–623]
Lower slices (msec)	1894 [1846–1939]	398 [364–425]	528 [494–558]	598 [564–633]
P-value	0.93	<0.001	0.21	0.36
Portal vein				
Upper slices (msec)	1858 [1812–1905]	361 [331–394]	500 [465–535]	573 [550–603]
Lower slices (msec)	1853 [1757–1918]	379 [344–412]	502 [478–534]	577 [546–609]
P-value	0.33	0.23	0.46	0.66
Vena Cava				
Upper slices (msec)	1737 [1665–1842]	369 [337–406]	524 [469–560]	558 [558–625]
Lower slices (msec)	1710 [1621–1801]	427 [401–459]	547 [504–579]	622 [579–648]
P-value	0.28	<0.001	0.02	0.02

Values are presented as median and IQR [25-percentile–75-percentile]. *P*-values are calculated using an unpaired Mann–Whitney test comparing T1 relaxation times measured on the two upper and two lower slices for the aorta, portal vein, and vena cava, as well as the left and right heart ventricle. ECV was calculated using the mean value of all liver and vessel segmentations precontrast and postcontrast ("mean all slices") or using liver and vessel T1 values of the slice at the level of the portal vein only ("single-slice portal vein level").

ECV Results

The ECV based on blood pool measurements in the aorta was significantly higher in patients with advanced fibrosis than in patients with early fibrosis at all time points, when measuring single-slice values at the level of the portal vein bifurcation (34.9% vs. 32.2% at 5 minutes, 34.9% vs. 33.1% at 10 minutes, and 36.0% vs. 33.9% at 15 minutes). Similar results were achieved when measuring the mean values of all four slices (35.4% vs. 33.3% at 5 minutes, 36.1% vs. 33.7% at 10 minutes, and 37.0% vs 34.9% at 15 minutes), as shown in Table 4. When the ECV was calculated based on blood pool measurements in the portal vein also all time points showed significant differences between the two patient groups for the single slice and the approach using the mean values of all four slices. In comparison, using the IVC as blood pool only 10 and 15 minutes results differed significantly between both groups while there was no significant difference in ECV values at 5 minutes (singe slice: 42.1% vs. 39.4%, $P = 0.074$ and mean all slices: 41.7% vs. 38.9%, $P = 0.062$). All single-slice ECV measurements (slices 1, 2, 3, and 4) are shown in the Table Figure S1 in the Supplemental Appendix.

The ROC analysis confirmed the good performance of ECV calculations in the aorta (mean of all slices) with an AUC = 0.72, CI 0.60–0.84 at 5 minutes, AUC = 0.73, CI 0.60–0.86 at 10 minutes, and AUC = 0.75, CI 0.63–0.86 at 15 minutes. When the ECV was calculated on a single slice, AUC was similar with an AUC = 0.72, CI: 0.60–0.84 at 5 minutes, AUC = 0.71, CI: 0.58–0.84 at 10 minutes, and AUC = 0.70, CI: 0.57–0.82 at 15 minutes (Fig. 3). No significant difference was found between the different AUC values (5 vs. 10 minutes $P = 0.91$; 5 vs. 15 minutes $P = 0.81$; 10 vs. 15 minutes $P = 0.91$). AUC values for the portal vein and IVC were comparable between the single slice and mean of all four slices approach with values of AUC = 0.70, CI: 0.58–0.83 for the portal vein single slice at 5 minutes, AUC = 0.67, CI 0.52–0.81 at 10 minutes, and AUC = 0.65, CI: 0.51–0.78 at 15 minutes, and mean of all slices AUC = 0.71, CI: 0.59–0.84, AUC = 0.72, CI 0.59–0.84 and AUC = 0.66, CI: 0.53–0.79 for 5, 10, and 15 minutes. Single slice ROC results for the IVC were for 5 minutes AUC = 0.63, CI: 0.49–0.77, 10 minutes AUC = 0.67, CI: 0.53–0.81, 15 minutes AUC = 0.66, CI: 0.53–0.79, and mean of all slices 5 minutes AUC = 0.68, CI: 0.53–0.84, 10 minutes AUC = 0.72, CI: 0.59–0.84, and 15 minutes AUC = 0.70, CI: 0.58–0.83.

Furthermore, ROC results of ECV were comparable with established laboratory biomarkers such as APRI score (AUC 0.66, CI 0.53–0.79) and FIB-4 (AUC 0.74, CI 0.63–0.87) (Fig. 4).

ROC results were poor for PDFF only to discriminate between F0-2 and F3-4 AUC 0.51 [CI: 0.38–0.65]. In a combined ROC using ECV of the Aorta (mean of all slices) with PDFF results were similar to ECV of the Aorta only

TABLE 4. ECV Values at Different Time Points

	5 minutes			10 minutes			15 minutes		
	F0-2	**F3-4**	***P***	**F0-2**	**F3-4**	***P***	**F0-2**	**F3-4**	***P***
Single-slice (portal vein level)									
Aorta (%)	32.2 [29.6–34.4]	34.9 [32.8–36.8]	0.002	33.1 [30.5–35.0]	34.9 [33.2–36.8]	0.004	33.9 [31.4–35.8]	36.0 [34.3–37.8]	0.005
Vena cava (%)	39.4 [37.4–42.5]	42.1 [38.0–45.2]	0.074	37.5 [34.0–39.3]	40.0 [36.8–42.7]	0.025	38.3 [34.3–41.9]	41.2 [37.9–43.8]	0.030
Portal vein (%)	30.5 [28.3–32.2]	32.8 [30.4–34.3]	0.005	31.8 [28.6–34.3]	33.6 [31.7–37.3]	0.016	32.9 [30.9–34.9]	34.9 [32.7–35.9]	0.042
Aorta and portal vein (%)	31.4 [29.0–34.7]	33.5 [31.1–35.0]	0.053	32.2 [28.8–34.0]	33.9 [31.5–37.8]	0.062	33.1 [31.2–34.9]	34.8 [33.4–36.2]	0.014
Mean all slices									
Aorta (%)	33.3 [30.8–34.8]	35.4 [33.1–37.6]	0.001	33.7 [31.6–34.7]	36.1 [34.2–37.5]	0.001	34.9 [32.2–36.0]	37.0 [34.8–39.2]	0.001
Vena cava (%)	38.9 [36.4–42.7]	41.7 [37.9–46.1]	0.062	37.0 [33.7–38.3]	39.3 [37.0–43.1]	0.002	38.0 [35.5–40.2]	40.0 [38.5–43.0]	0.004
Portal vein (%)	30.6 [28.1–32.8]	33.1 [30.9–34.7]	0.002	31.8 [28.6–34.3]	33.6 [31.7–37.3]	0.016	33.2 [31.2–35.1]	34.9 [32.8–36.6]	0.028
Aorta and portal vein (%)	31.4 [28.4–34.1]	33.6 [31.9–35.3]	0.011	32.2 [28.8–34.0]	33.9 [31.5–37.8]	0.062	33.5 [31.5–35.2]	35.2 [33.4–37.1]	0.012

Values are presented as median and IQR [25-Percentile–75-Percentile] or *n*. *P*-values are calculated using an unpaired Mann–Whitney test, comparing patients with liver fibrosis grades F0-2 and patients with liver fibrosis grade 3–4. ECV was calculated using the mean value of all liver and vessel segmentations precontrast and postcontrast ("mean all slices") or using liver and vessel T1 values of the slice at the level of the portal vein only ("single-slice portal vein level"). ECV with aorta and portal vein as blood pool was calculated with a 30% weighting of the arterial blood pool and 70% weighting of the portal venous blood pool.
ECV = extracellular volume fraction.

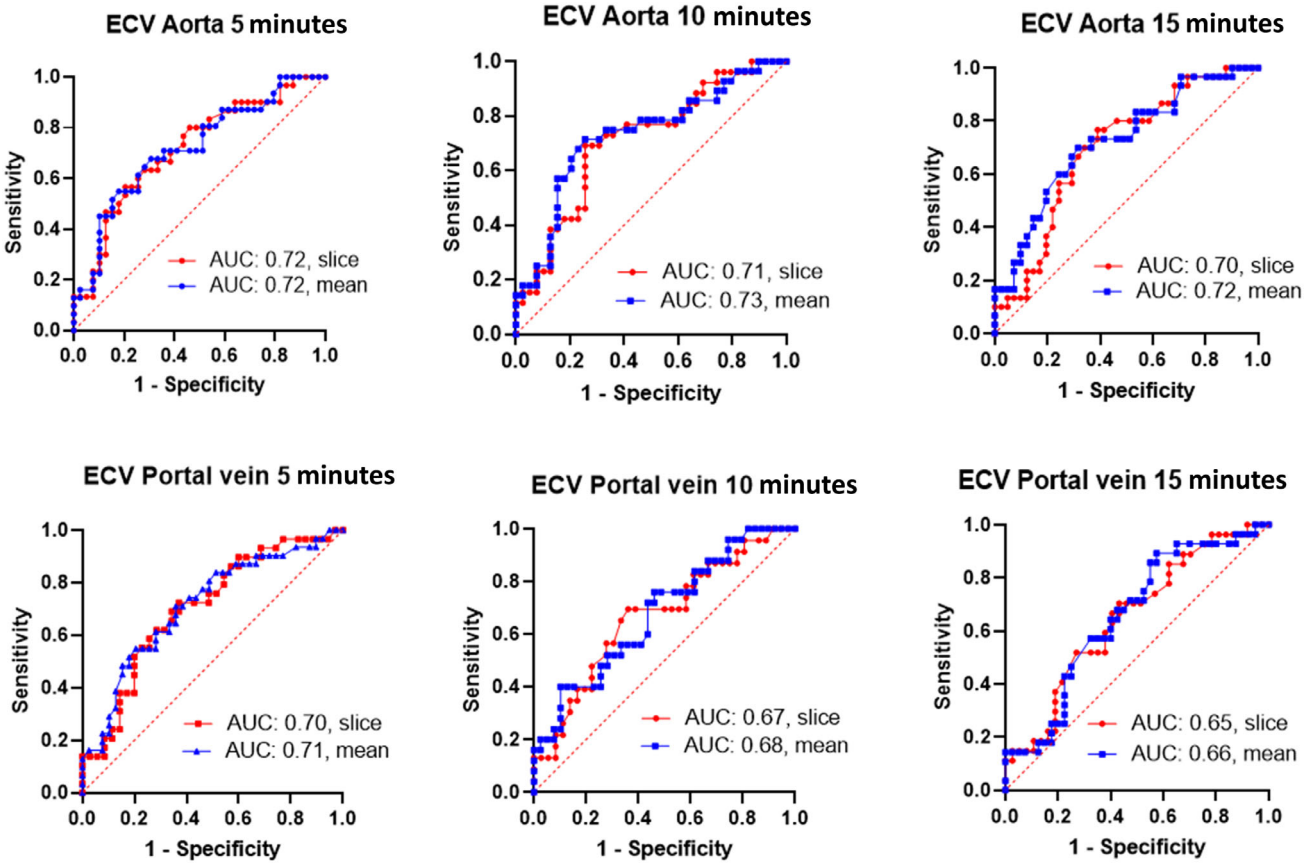

FIGURE 3: ROC analysis. Calculating ECV using the blood pool measurements from the aorta has higher AUC than using the blood pool from the portal vein. Discrimination between F0-2 and F3-4 is highest when the ECV was calculated as the mean value of four slices and blood pool measurements in the aorta (AUC = 0.76).

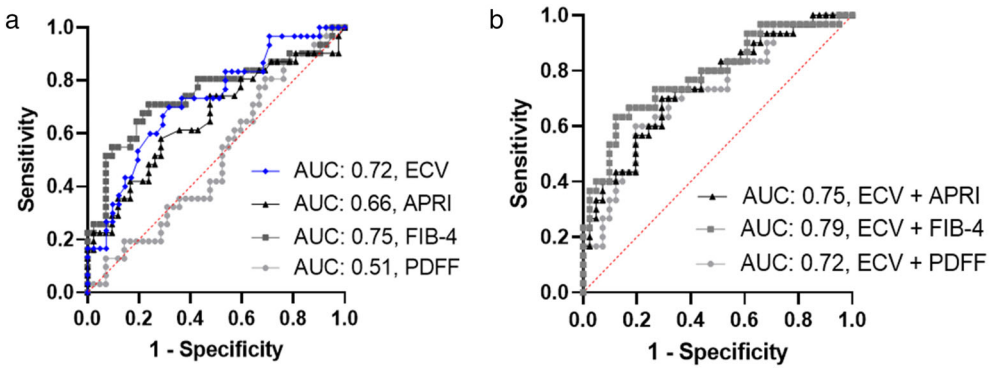

FIGURE 4: ROC analysis. In (a) is shown that using FIB-4 score has the highest AUC to discriminate between F0-2 and F3-4 (0.75), followed by the ECV using the blood pool measurements from the Aorta after 15 minutes (mean value of all four slices). AUC results of APR (0.66) and PDFF (0.51) are much lower. In (b) combined ROC analysis results from Aorta 15 minutes (mean value of all four slices) combined with APRI (AUC = 0.75), FIB-4 (AUC = 0.79), and PDFF (AUC = 0.72) are shown.

(0.72 vs. 0.72 for 5 minutes, 0.74 vs. 0.73 for 10 minutes, and 0.72 vs. 0.72 for 15 minutes, Fig. 5). Further, stratified AUC analysis for ECV identifying patients with F3-4 in the subgroups without hepatic statosis (PDFF <5%) and patients with at least mild steatosis (PDFF >5%) show similar results than for the total study population (Fig. S1 in the Supplemental Material).

Reproducibility Analysis

Inter-rater reproducibility based on ICC was excellent for T1 mapping in the liver precontrast (0.99) and postcontrast (0.99 for all time points), as well as for measurements in the aorta precontrast (0.99) and postcontrast (0.99). Furthermore, ICCs for ECV measurements were excellent as well (0.98–0.99).

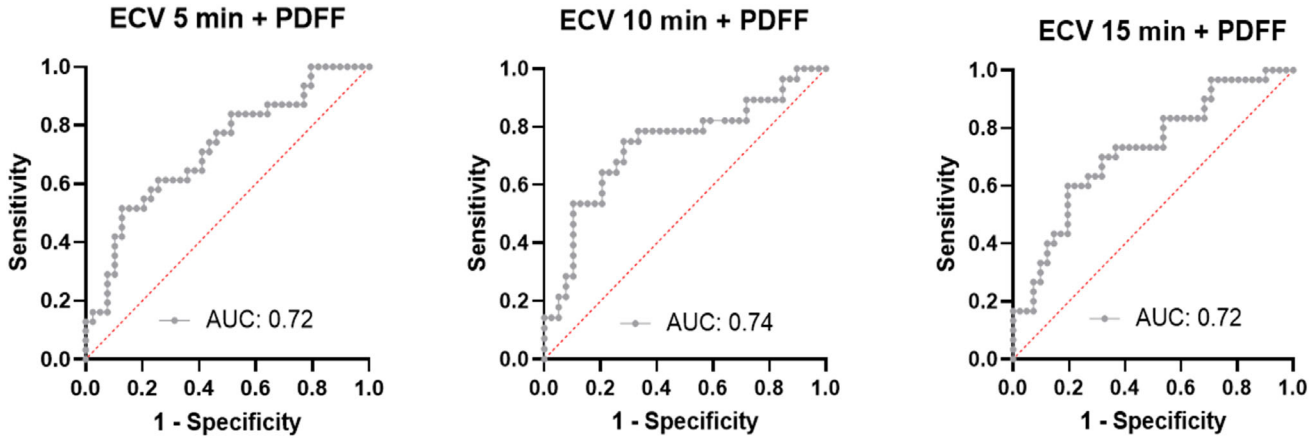

FIGURE 5: ROC Analysis ECV Aorta 5, 10, and 15 minutes combined with PDFF results. Combining ECV with PDFF results in similar AUC as without PDFF (see also Fig. 3) at 5 minutes AUC = 0.72, 10 minutes, AUC = 0.74 and 15 minutes AUC = 0.72.

Discussion

This study showed that ECV is higher in patients with histology-proven advanced liver fibrosis than in patients with early liver fibrosis using the blood pool measurements from the aorta, the IVC and the portal vein at 5, 10, and 15 minutes. However, significant differences between the upper and lower slices of the blood bool measurement were observed at the earliest time point (5 minutes), indicating a potentially more robust measurement at equilibrium phase, notable when comparing measurements between different slices.

Our results showed that ECV values are most reliable when the liver T1 was normalized with the blood pool T1 in the aorta, while the best ECV performance was achieved at 15 minutes by averaging over four slices. However, a less time-consuming single-slice approach showed good performance as well and may be used in shorter MRI protocols using the 10 minutes or 5 minutes postcontrast time point.

As the T1 of the liver and blood pool change over time between slices due to a contrast wash-out effect, a single-slice approach may be more appropriate for earlier time points at 5 minutes. At this time point, a rapid contrast washout from the liver and vessels occurs, while this washout effect is less pronounced at 10–15 minutes, when equilibrium phase has been reached. However, no significant differences were found between the different time points of ECV calculations and between the averaging and single-slice approach.

The liver extracellular space consists of an intravascular space with liver vessels and sinusoids, the biliary tracts, as well as the interstitial space with extracellular matrix, eventual inflammatory infiltrates, and collagen deposition in fibrosis.[31] The underlying hypothesis for ECV calculation is that within a given time for equilibration, an extracellular contrast agent will diffuse through tissues to reach roughly equal concentrations within the intravascular space in the blood pool measurements and the interstitial space of the liver, while the biliary tracts are neglected.[14] Liver fibrosis is associated with an expansion of the interstitial space secondary to the deposition of collagen and matrix proteins produced by fibrogenic cell populations in response to tissue injury.[32] This results in distortion of the normal hepatic architecture and impaired liver function.[33] The consequence of this distortion and extension of the interstitial space is an increased accumulation of extracellular MRI contrast agent in the space of Disse, which is reflected by an increased ECV.[34] As the liver sinusoidal endothelial cells are fenestrated, an early equilibrium phase is obtained already at 5 minutes, reflecting both the vascular space with the liver sinusoids and the extracellular matrix in the space of Disse.[35] Whether a later measurement at 10–15 minutes is more weighted for the extravascular interstitial space, due to a washout effect of the contrast agent from the liver sinusoid, warrants further investigations.

Studies reporting ECV of the liver are still scarce but mostly use blood pool measurements on a single slice of T1 maps in the aorta.[20–22,36] One study by Jin et al. used mean liver and aortic measurements from three consecutive slices,[18] but no study compared single-slice and multislice measurements. Based on our results and given that every T1 mapping slice has an acquisition time of roughly 30 sec (one breath hold), the additional scan time needed for four slices instead of one slice may not be justified for mean liver ECV calculations. However, the multislice ECV calculation may be helpful if calculation of segmental ECV or if ECV of solid liver lesions is intended. Furthermore, ECV calculations based on blood pool measurements in the portal vein and IVC is possible but limited related to slice acquisitions where the portal vein is visualized and by a mixture phenomenon with significant differences of the measured T1 values above and below the liver vein confluence as shown in Table 3. In addition, the IVC may be slim in some patients. The aortic location thus might ensure the most reliable measurements.

Our findings corroborate and extend the findings of other studies.[14,18,21,22] A first MRI study investigating liver ECV was performed in a preclinical setting in 2018, showing a higher ECV in advanced liver fibrosis in rats.[14] One of the first clinical studies showed higher ECV values in patients

with chronic hepatitis B and more advanced stages of fibrosis (F0 = 20.3%, F1 = 23.4%, F2 = 24.0%, F3 = 28.3%, and F4 = 32.9%),[18] with better performance for liver fibrosis staging than APRI and FIB-4.[20] This group used another T1 mapping technique (3D gradient echo acquisitions) with a bit lower, but nevertheless comparable ECV values in relation to our results, with an ECV of 36.9% in patients with liver fibrosis grade F3-4 and an ECV of 33.3% in patients with liver fibrosis grade F0-2. In studies with similar T1 mapping techniques based on a MOLLI sequence but different patient populations, significantly higher ECV was found.[21,22] ECV was significantly higher in patients with primary sclerosing cholangitis and fibrosis grades F ≥ 2 (30.5% ± 4.4%) than in patients with fibrosis grades F0-1 (26.3% ± 1.9%) at 10 minutes after contrast administration.[22] The same group could show in another publication that ECV was significantly higher in patients with AIH and fibrosis grade F2-4 (38.7% ± 18.9%), as compared with fibrosis grade F0-1 (27.1% ± 3.2%).[21] Similar to our observations, Luetkens et al. found no significant difference in ECV measurements between 5 and 25 minutes.[17]

Limitations

One major limitation of this study is the small subgroup size of patients with early fibrosis grade 0 and 1 and in the advanced fibrosis group the small number of patients with cirrhosis grade 4. However, the patient population is well characterized with liver MRI and biopsy within less than 3 month and hematocrit measurements on the day of MRI.

The T1 relaxation times are influenced by the presence of steatosis and inflammation.[6] However, there was no significant difference in BMI and liver steatosis amount between patients with early and advanced liver fibrosis. Second, liver T1 measurements included both liver parenchyma and small vessels and, therefore, some partial volume effects, even if the liver border, large vessels, and major bile ducts were rigorously excluded. The results should therefore be validated in a larger patient population, including more patients with very early (F0-1) and very advanced (F4) liver fibrosis and allowing further subgroup categorization based on amount of steatosis and activity.

Conclusion

Liver ECV is significantly higher in advanced liver fibrosis compared to early liver fibrosis with blood pool measurements performed in the aorta, IVC, and portal vein at 5, 10, and 15 minutes. However, a smaller variability was observed for blood pool measurements between slices at 15 minutes.

Acknowledgment

Open access funding provided by Inselspital Universitatsspital Bern.

References

1. Mansour D, McPherson S. Management of decompensated cirrhosis. Clin Med (Lond) 2018;18(Suppl 2):s60-s65.
2. Campana L, Iredale JP. Regression of liver fibrosis. Semin Liver Dis 2017;58(1):1-10.
3. Poynard T, Lenaour G, Vaillant JC, et al. Liver biopsy analysis has a low level of performance for diagnosis of intermediate stages of fibrosis. Clin Gastroenterol Hepatol 2012;10(6):657-663.e657.
4. Obmann VC, Mertineit N, Berzigotti A, et al. CT predicts liver fibrosis: Prospective evaluation of morphology-and attenuation-based quantitative scores in routine portal venous abdominal scans. PloS One 2018; 13(7):e0199611.
5. Obmann VC, Marx C, Hrycyk J, et al. Liver segmental volume and attenuation ratio (LSVAR) on portal venous CT scans improves the detection of clinically significant liver fibrosis compared to liver segmental volume ratio (LSVR). Abdom Imaging 2020;46(5):1912-1921.
6. Obmann VC, Mertineit N, Marx C, et al. Liver MR relaxometry at 3T–segmental normal T1 and T2* values in patients without focal or diffuse liver disease and in patients with increased liver fat and elevated liver stiffness. Sci Rep 2019;9(1):8106.
7. Zhang YN, Fowler KJ, Boehringer AS, et al. Comparative diagnostic performance of ultrasound shear wave elastography and magnetic resonance elastography for classifying fibrosis stage in adults with biopsy-proven nonalcoholic fatty liver disease. Eur Radiol 2022;32(4): 2457-2469.
8. Osman AM, El Shimy A, Abd El Aziz MM. 2D shear wave elastography (SWE) performance versus vibration-controlled transient elastography (VCTE/fibroscan) in the assessment of liver stiffness in chronic hepatitis. Insights Imaging 2020;11(1):38.
9. Lefebvre T, Wartelle-Bladou C, Wong P, et al. Prospective comparison of transient, point shear wave, and magnetic resonance elastography for staging liver fibrosis. Eur Radiol 2019;29(12):6477-6488.
10. Venkatesh SK, Yin M, Ehman RL. Magnetic resonance elastography of liver: Technique, analysis, and clinical applications. J Magn Reson Imaging 2013;37(3):544-555.
11. Singh S, Venkatesh SK, Wang Z, et al. Diagnostic performance of magnetic resonance elastography in staging liver fibrosis: A systematic review and meta-analysis of individual participant data. Clin Gastroenterol Hepatol 2015;13(3):440-451.e446.
12. Horowitz JM, Venkatesh SK, Ehman RL, et al. Evaluation of hepatic fibrosis: A review from the society of abdominal radiology disease focus panel. Abdom Imaging 2017;42:2037-2053.
13. Flett AS, Hayward MP, Ashworth MT, et al. Equilibrium contrast cardiovascular magnetic resonance for the measurement of diffuse myocardial fibrosis: Preliminary validation in humans. Circulation 2010;122(2): 138-144.
14. Luetkens JA, Klein S, Träber F, et al. Quantification of liver fibrosis at T1 and T2 mapping with extracellular volume fraction MRI: Preclinical results. Radiology 2018;288(3):748-754.
15. Moon JC, Messroghli DR, Kellman P, et al. Myocardial T1 mapping and extracellular volume quantification: A Society for Cardiovascular Magnetic Resonance (SCMR) and CMR working Group of the European Society of cardiology consensus statement. J Cardiovasc Magn Reson 2013;15:92.
16. De Meester De Ravenstein C, Bouzin C, Lazam S, et al. Histological validation of measurement of diffuse interstitial myocardial fibrosis by myocardial extravascular volume fraction from modified look-locker imaging (MOLLI) T1 mapping at 3 T. J Cardiovasc Magn Reson 2015; 17(1):48.
17. Luetkens JA, Klein S, Träber F, et al. Quantification of liver fibrosis: Extracellular volume fraction using an MRI bolus-only technique in a rat animal model. Eur Radiol Exp 2019;3(1):22.
18. Jin K, Wang H, Zeng M, et al. A comparative study of MR extracellular volume fraction measurement and two-dimensional shear-wave elastography in assessment of liver fibrosis with chronic hepatitis B. Abdom Radiol 2019;44(4):1407-1414.

19. Lyu L, Liu X-L, Rui M-P, et al. Liver extracellular volume fraction values obtained with magnetic resonance imaging can quantitatively stage liver fibrosis: A validation study in monkeys with nonalcoholic steatohepatitis. Eur Radiol 2020;30(10):5748-5757.

20. Wang HQ, Jin KP, Zeng MS, et al. Assessing liver fibrosis in chronic hepatitis B using MR extracellular volume measurements: Comparison with serum fibrosis indices. Magn Reson Imaging 2019;59:39-45.

21. Mesropyan N, Kupczyk P, Dold L, et al. Non-invasive assessment of liver fibrosis in autoimmune hepatitis: Diagnostic value of liver magnetic resonance parametric mapping including extracellular volume fraction. Abdom Radiol 2021;46(6):2458-2466.

22. Mesropyan N, Kupczyk P, Kukuk GM, et al. Diagnostic value of magnetic resonance parametric mapping for non-invasive assessment of liver fibrosis in patients with primary sclerosing cholangitis. BMC Med Imaging 2021;21(1):65.

23. Zech CJ, Ba-Ssalamah A, Berg T, et al. Consensus report from the 8th international forum for liver magnetic resonance imaging. Eur Radiol 2020;30(1):370-382.

24. Bedossa P, Poitou C, Veyrie N, et al. Histopathological algorithm and scoring system for evaluation of liver lesions in morbidly obese patients. Hepatology 2012;56(5):1751-1759.

25. Bedossa P, Poynard T. An algorithm for the grading of activity in chronic hepatitis C. Hepatology 1996;24(2):289-293.

26. Schelbert EB, Messroghli DR. State of the art: Clinical applications of cardiac T1 mapping. Radiology 2016;278(3):658-676.

27. Mesropyan N, Isaak A, Faron A, et al. Magnetic resonance parametric mapping of the spleen for non-invasive assessment of portal hypertension. Eur Radiol 2021;31(1):85-93.

28. R Core Team. *R language definition*. Vienna: R Foundation for Statistical Computing; 2000.

29. Venkatesh SK, Xu S, Tai D, Yu H, Wee A. Correlation of MR elastography with morphometric quantification of liver fibrosis (fibro-C-index) in chronic hepatitis B. Magn Reson Med 2014;72(4):1123-1129.

30. Koo TK, Li MY. A guideline of selecting and reporting Intraclass correlation coefficients for reliability research. J Chiropr Med 2016;15(2):155-163.

31. Martinez-Hernandez A, Amenta PS. The hepatic extracellular matrix. I. Components and distribution in normal liver. Virchows Arch A Pathol Anat Histopathol 1993;423(1):1-11.

32. Acharya P, Chouhan K, Weiskirchen S, Weiskirchen R. Cellular mechanisms of liver fibrosis. Front Pharmacol 2021;12:671640.

33. Lee YA, Wallace MC, Friedman SL. Pathobiology of liver fibrosis: A translational success story. Gut 2015;64(5):830-841.

34. Mesropyan N, Kupczyk PA, Dold L, et al. Assessment of liver cirrhosis severity with extracellular volume fraction MRI. Sci Rep 2022;12(1):9422.

35. Drew L. Tipping the balance. Nature 2018;564(7736):S74-s75.

36. Kupczyk PA, Mesropyan N, Isaak A, et al. Quantitative MRI of the liver: Evaluation of extracellular volume fraction and other quantitative parameters in comparison to MR elastography for the assessment of hepatopathy. Magn Reson Imaging 2021;77:7-13.